Electronic Supplementary Material (ESI) for Soft Matter.

Supporting Information

Contrast variation SANS measurement of shell monomer profiles of smart acrylamide-based core-shell microgels

Marian Cors[1, 2], Lars Wiehemeier[1], Oliver Wrede[1], Artem Feoktystov[3], Fabrice Cousin[4], Thomas Hellweg[1*], Julian Oberdisse[2*]

[1] *Department of Physical and Biophysical Chemistry, Bielefeld University, Universitätsstr. 25, 33615 Bielefeld, Germany*
[2] *Laboratoire Charles Coulomb (L2C), University of Montpellier, CNRS, 34095 Montpellier, France.*
[3] *Forschungszentrum Jülich GmbH, Jülich Centre for Neutron Science JCNS at Heinz Maier-Leibnitz Zentrum MLZ, 85748 Garching, Germany.*
[4] *Laboratoire Léon Brillouin, UMR 12 CEA/CNRS, CEA Saclay, 91191 Gif Sur Yvette, France*

* *Authors for correspondence : thomas.hellweg@uni-bielefeld.de, julian.oberdisse@umontpellier.fr*

Swelling behavior of a pNIPMAM-pNNPAM microgel

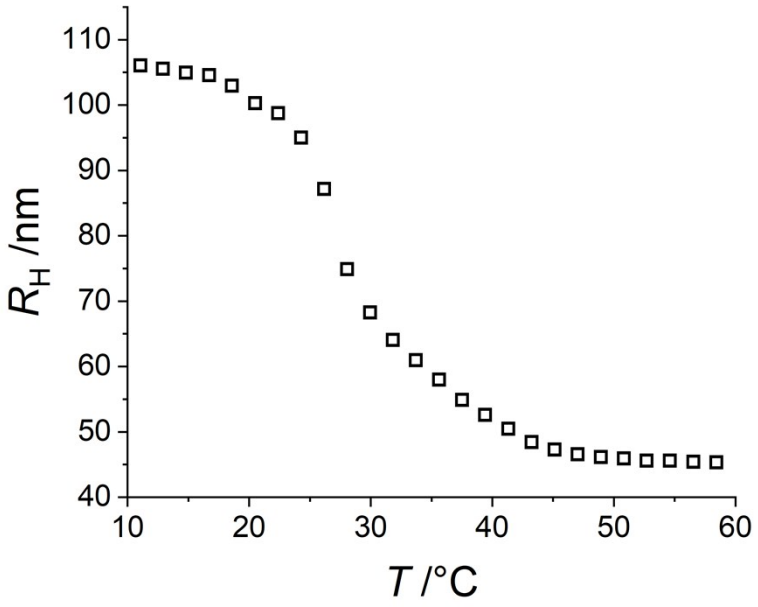

Figure S1: Swelling curve of a H-pNIPMAM D7-pNNPAM core-shell microgel with a CCC of 5 mol% measured in water by PCS.

Possible models for core-shell geometries

Core and core-shell geometries have been described in the literature and reviewed by us in a previous article,[1] Figure 9.They include box profiles, fuzzy interfaces, the thermodynamic Boon-Schurtenberger model, and the multi-shell approach of Pedersen and ourselves.

For core shells, the simplest shell geometry is the hollow sphere geometry shown in Figure S2. By volume conservation of monomers, the constant density in the shell is directly related to its volume (which itself depends on the thickness), the product must be constant. From the one-dimensional density profile, the scattered intensity I(q) can be found using the corresponding 3D Fourier transform for spherical symmetry, if the concentration is low and known, as detailed in our previous article,[1] relating the volume fraction profile to the scattering length density:

$$\rho(r) = \rho_{Mono} \cdot \Phi(r) + \rho_{Solv} \cdot (1 - \Phi(r))$$

This confers contrast to the microgel in the solvent, $\Delta\rho(r) = \rho(r) - \rho_{Solv}$, and gives rise to the scattered intensity I(q):

$$I(q,r) = \frac{N}{V}\left[\int 4\pi r^2 \Delta\rho(r)\frac{sin(qr)}{qr}dr\right]^2$$

Here N/V is the number of microgels per volume chosen to satisfy the concentration of monomer volume. In our reverse Monte-Carlo (RMC) implementation, we translate the last equation into a discrete sum over the shells, with the radial variable r given by the number of the shell i, thus the outer radius of each shell r(i) = iΔR:

$$I_{RMC}(q,r,n) = \sum_{i=1}^{N_p}\frac{N}{V}\left[\frac{4\pi}{3}r(i)^3(\Delta\rho(i) - \Delta\rho(i+1))3\frac{sin(qr) - qrcos(qr)}{(qr)^3}\right]^2$$

Here $\Delta\rho(i)$ is the scattering length contrast of shell i, and the contrast of the surrounding solvent shell $\Delta\rho(N_p+1)$ is set to zero.

Coming back to the hollow sphere and by definition of the radius of gyration, which under spherical symmetry is an integral weighting the local density, R_g must lie between the inner and the outer radius, see Figure S2. This simple geometrical argument allows us to exclude this geometry by comparison with the experimentally observed Guinier domain.

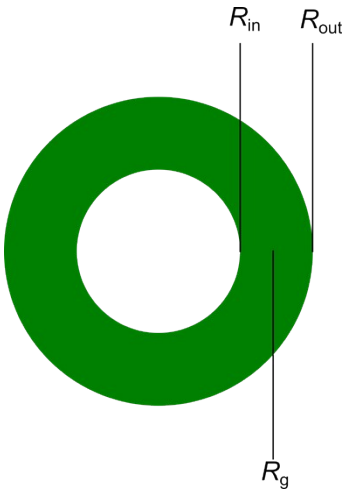

Figure S2: Geometry of a hollow shell with the inner radius (R_{in}), outer radius (R_{out}) and approximately the radius of gyration (R_g).

The idea of the modeling part associated with Figure 2 was to propose the following 'educated guesses' for the geometry (and thus density profile), calculate the corresponding I(q), and confront it with the experiment

in Figure 2a. The result was that all 'intuitive' shell models fail, and the centered ones approach the true geometry.

Core-Shell: Shell polymer located just outside the known core profile (decaying at 28 nm) with a maximum total density identical to the one of the core, thus setting the thickness by shell monomer volume conservation.

$$\Phi_{shell}(r) = 0 \ (r<28nm)$$

$$\Phi_{shell}(r) = \Phi_{core(max)}\ (r) - \Phi_{core}\ \ (r) (r>28\ nm)$$

$$\Phi_{shell}(r) = 0 \text{ (outside set by volume conservation)}$$

Shell-IPN: This ad-hoc model is similar to the core-shell model with an increased interpenetration into the core producing smaller shells, in order to see if a better agreement with experimental intensity (Figure 2a) is obtained. This is the case but it is not sufficient to describe the data. The density profile obeys the same equation as the core-shell model above, with the 28 nm internal radius reduced to 10 nm. The agreement with the intensity is better but still not satisfactory.

Centered: Given the too big size of the above models as compared to the measurement, as many shell monomers as possible have been fit into the centre of the particle. Filling the remaining space with shell monomers, starting from the centre, setting the total volume fraction to $\Phi = 1$, gives the following shell monomer volume fraction profile:

$$\Phi_{shell}(r) = 1 - \Phi_{core}(r) \quad (r < \text{radius set by volume conservation})$$

$$\Phi_{shell}(r) = 0 \qquad (r > \text{radius set by volume conservation})$$

Note that the last (outmost) shell may be only partially filled with the remaining monomers defined by volume conservation. This explains the non-perfect steepness of this profile at the particle surface.

High-*q* analysis

The high-*q* slopes of the performed SANS measurements for different temperatures of a pNIPMAM-pNNPAM core-shell particle in Figure 3 in the article are reported here. They indicate dominant shell chain scattering at low temperature in the swollen state, and dominant interface (close to Porod) scattering in the collapsed state, presumably with some remaining chain contributions.

Temperature	**Slope**
15°C	1.5
30°C	4.0
35°C	3.8
40°C	3.6
55°C	3.2

Table S1: High-q slopes of H/D pNIPMAM-pNNPAM core-shell particles with matched core as a function of temperature, for core crosslinking of 10 mol%.

Similarly, for the different cross-linker concentrations of the core and unchanged crosslinking of the shell (1.9 mol%) in Figure 4, we find at 55°C:

Core cross-linking	**Slope**
5 mol%	2.2
10 mol%	3.2
15 mol%	2.7

Table S2: High-q slopes of H/D pNIPMAM-pNNPAM core-shell particles with matched core as a function of core crosslinking at 55°C.

Radial core and shell monomer distribution

Figure 4 in the main article shows the radial shell monomer density at 15, 35 and 55 °C. In Figure S3 $r^2\Phi$ is plotted as a function of the radius r.

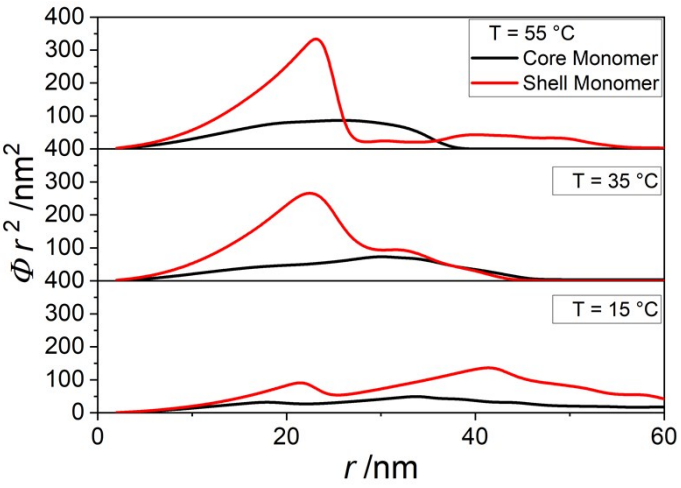

Figure S3: $r^2\Phi$ as a function of the radius of the pNNPAM shell monomer density of a pNIPMAM-pNNPAM core shell microgel particle with a CCC of 10 mol% at different temperatures.

References

(1) Cors, M.; Wiehemeier, L.; Hertle, Y.; Feoktystov, A.; Cousin, F.; Hellweg, T.; Oberdisse, J. Determination of Internal Density Profiles of Smart Acrylamide-Based Microgels by Small-Angle Neutron Scattering: A Multishell Reverse Monte Carlo Approach. *Langmuir* **2018**, *34*, 15403–15415.